PROCEEDINGS OF SCIENCE

# Interplanetary shocks manifestation in cosmic rays and geomagnetic field

**L.P. Shadrina**
*Academy of Sciences of Republic of Sakha (Yakutia)*
*33 Lenin ave., 677007 Yakutsk, Russia*
*e-mail: lushard@mail.ru*

**G.F. Krimsky, I.Ya. Plotnikov, S.A. Starodubtsev, I.S. Petukhov***
*Yu.G. Shafer Institute of Cosmophysical Research and Aeronomy of SB RAS*
*31 Lenin ave., 677980 Yakutsk, Russia*
*e-mail:krymsky@ikfia.sbras.ru, plotnikov@ikfia.sbras.ru, starodub@ikfia.sbras.ru, i_van@ikfia.sbras.ru*

The analysis of ground based measurements of cosmic ray intensity and geomagnetic field during the 96 interplanetary shocks passing by Earth was fulfilled. It was shown that most part of the shocks (43 of 96) were accompanied by simultaneous effects – decreases in the cosmic ray intensity and geomagnetic field. But there was no amplitude accordance: more part of the strong and moderate geomagnetic storms with amplitude more then 60 nT (44 from 60) did not observed together with the cosmic ray intensity decreases or these effects were very week. Nearly a half of the shocks (46 of 96) had effects only in cosmic ray or in geomagnetic field, and 7 shocks had no any ground effects. The difference of our approach consists that our purpose is to clarify the role of the geometrical factor of moving solar wind structure intersections respect to the Earth by the ratio of their geoeffective manifestations in the geomagnetic field and in the cosmic rays. Thus were obtained new data confirming our preliminary conclusions that the region responsible for the generation of geomagnetic storms and cosmic ray Forbush decreases of are spatially separated in the interplanetary disturbances.

*The 34th International Cosmic Ray Conference*
*30 July- 6 August, 2015*
*The Hague, The Netherlands*

*Speaker



PoS(ICRC2015)111

## 1.Introduction

Question of the geoeffectiveness ratio of various solar wind structures, despite of the big number of papers on this topic is still open. On the one hand, statistical analysis of the geomagnetic field depression showed that geomagnetic storms are generated by the passage of interplanetary shocks, magnetic clouds (MC), sheath, coronal mass ejection (CME), compression regions at the boundary of the slow and fast streams (corotating interaction regions CIR) etc. [1, 3, 5, 6, 14]. On the other hand, mentioned heliospheric disturbances structures modulate the cosmic rays (CR) distribution, which manifests at the ground as their intensity depression [4, 7, 10]. Geomagnetic storms are the result of some sort of "point of interaction" – their occurrence and intensity mainly depends on the IMF structure (southward Bz component) at the point of interaction of interplanetary disturbance and Earth's magnetosphere. This is one side of the geoeffectiveness. Cosmic rays in addition to the geoeffectiveness (i.e. CR intensity decreases on the ground), are gelioeffectiveness Since the CR intensity decrease is due to the prohibited area for their trajectory in the heliospheric disturbance so that a region with a low content of CRs appears in interplanetary space. So geomagnetic storm geoeffectiveness has a local character, whereas Fobush-effect gelioeffectiveness reflects the influence of dynamical processes in interplanetary space. Analysis of interplanetary disturbances geoeffectiveness on their manifestations in CR and geomagnetic-field is presented in papers [8] and [11]. The authors consider the possibility of a joint consideration of CR and the Dst data in order to find a precursor of heliospheric disturbance come near the Earth. The difference of our approach is that we aim to clarify the role of the geometrical factor of moving solar wind structure intersections respect to the Earth by the ratio of their geoeffective manifestations in the geomagnetic field and CR.

The aim of this paper is to estimate efficiency ratio of interplanetary shock on the Dst index decreases (geomagnetic storms, GSt) and CR intensity variations at Yakutsk station (Forbush decreases, FD).

## 2.Data

A list of interplanetary shocks (IPS) related with CME from paper [9] during 6 years (1997-2002) on the growth phase of 23 solar cycle was used as a basis for investigations. As the indicator for the geomagnetic storms there was used Dst index of geomagnetic field, and for the Forbush-decreases – isotropic component of galactic cosmic ray (CR) intensity calculated by global survey method proposed and developed in ShICRA of SB RAS.

We considered four types of IPS geophysical responses:

1. simultaneous registration (with a scatter of less than 24 hours) of CR intensity and geomagnetic field decreases, geomagnetic storm and Forbush-decrease (GSt + FD);
2. the response in only one of these parameters – storm without Forbush-decrease (GSt – FD)
3. or Forbush-decrease without storm (FD – GSt);
4. the events when the passage of IPS have no significant response as a decrease neither in the geomagnetic field, nor in the isotropic component of CR intensity (– GSt – FD).

The investigated time interval is in the first half of the 23rd solar cycle. The minimum of the cycle was observed in 1996 (annual average sunspot number W = 8,6), the maximum – in

2000 (W = 119,6). Number of IPS varies synchronously with solar activity (Fig. 1): it increases at the ascending phase, reaches a maximum at the maximum of the cycle and decreases at the declining phase. 25 of 96 shocks (over a quarter) occurs at the year of solar activity maximum.

The distribution of these 96 IPS for the four described above types of geoeffective responses is: 43 events (44,8%) – storms with Forbush decreases (St + F), 38 events (39,6%) – storms without Forbush decreases (St – F), 8 events (8,3%) – Forbush decreases without storms (F – St) and in 7 cases there are no geoeffective events ( – St – F) (7,3%) (Fig. 2). Thus, we can write the ratio of geoeffectiveness (F – St) : (St + F) : (St – F) : ( – St – F) as 1,0 : 4,8 : 5,4 : 0,9. In paper [2] such events were studied for the period 1968-1974 and here was obtained ratio of geoeffectiveness for 3 first groups of responses: 1 : 4 : 5. I.e. in 23-th solar cycle the number of simultaneous events in the geomagnetic field and the RC is more often than in the 20-th cycle.

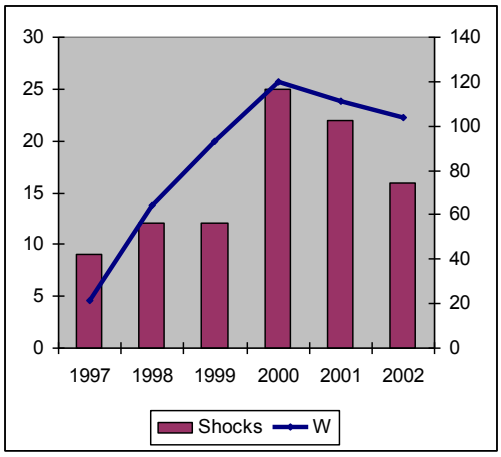


**Figure 1:** The number of shock waves (columns, left scale) in the beginning of 23rd solar cycle (W - Wolf number, right scale).

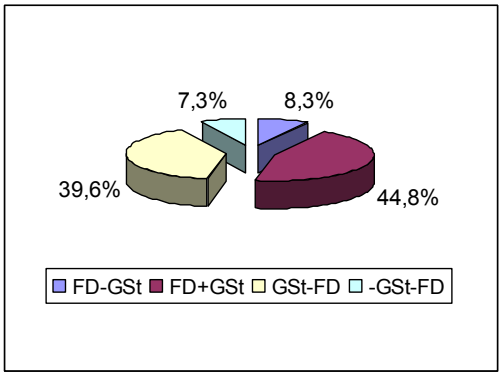


**Figure 2:** The ratio of four types geoeffective responses in 1997-2002.

It is known that storms and CR-Forbush decreases usually are characterized by the value of Dst index and the relative variation δI/I in the main phase of the events. According to the accepted classification [1], we consider storms with Dst < –100 нТл as a big (intense) geomagnetic storm (bGSt), as a moderate one (mGSt) for –100 < Dst < –60 нТл and as a small storm (sGSt) for –60 < Dst < –30 нТл). Similarly CR Forbush decrease we consider as a big (bFD) for δI/I > 7%, as a moderate (mFD) for 4% < δI/I < 7% and as a small (sFD) for 1,5% < δI/I < 4 %. If the response in the geomagnetic field and in the CR intensity is not observed we

denote this event as no (n). Thus, from 96 IPSs during the considered time interval we formed 16 types of the events: from (bGSt, bFD) to (nGSt, nFD). The corresponding distribution is shown in Table 1.

The big geomagnetic storms accompanied by small CR intensity decreases were observed more often (Tabl. 1): 17 events (bGSt, sFD – 17,7%). Quite often, there are events of geomagnetic storms without Forbush decreases – a total of 38 events, including 10 big storms (bGSt, nFD – 10,4%), 13 moderate storms (mGSt, nFD – 13,5%) and 15 small storms (sGSt, nFD – 15,6%). This statistics and classification agrees with the results for the time interval 1982-2002 in paper [8], who found 28% of the events in Dst without significant cr decreases (here 24%) and 19% CR decreases without Dst changes (here 8%).

Table 1. The frequency of occurrence $n_{ij}$ of 16 types of the events with various intensity in the geomagnetic field (GSt) and in the cosmic ray intensity (FD) – big, moderate, small or no.

| Dst / δI/I | bGSt | mGSt | sGSt | nGSt |
|---|---|---|---|---|
| **bFD** | **6** | **0** | **0** | **0** |
| **mFD** | **6** | **4** | **1** | **2** |
| **sFD** | **17** | **4** | **5** | **6** |
| **nFD** | **10** | **13** | **15** | **7** |

### 3. The analysis of statistical data of the table 1

The values of the two-dimensional random quantity $n_{ij}$ (GSt, FD) compares with a set of matrices $N_{ij}$, calculated according to the formula of binormal probability density:

$$p(x,y)=\exp\left(-\frac{(x-\mu_1)^2/2\sigma_1^2+(y-\mu_2)^2/2\sigma_2^2-(x-\mu_1)(y-\mu_2)/\sigma_1\sigma_2}{1-\rho^2}\right)/2\pi\sqrt{1-\rho^2}\sigma_1\sigma_2 \qquad (1)$$

for $x_i$ = {<nSt>, <sSt>, <mSt>, <bSt>} и $y_j$ = {<nF>, <sF>, <mF>, <bF>} and for set of the free parameters in the range (0 ÷ ∞): mathematical expectations $\mu_1$ and $\mu_2$, and dispersions $\sigma_1$ and $\sigma_2$, and the correlation coefficient ρ between the components of two dimensional random variable (x, y) in the range (-1 ÷ 1).

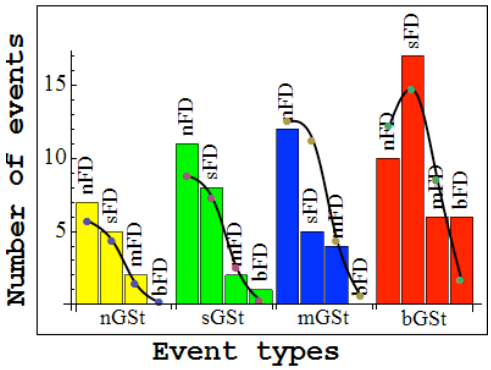


**Figure 3:** The frequency distribution of 16 types of the events and the best approximation calculated by formula (1) for two-dimensional random variable (GSt, FD).

Figure. 3 shows the frequency distribution of the 16 types of the events and their best approximation calculated by the formula (1), normalized to the setpoint $x_i$ = {15; 45; 80; 200} and $y_j$ = {0.75; 2.75; 5.5; 10.0}. The values of the five free parameters ($\mu_1$ = 150±15, $\mu_2$ = 2±0.5, $\sigma_1$ = 91±5, $\sigma_2$ = 3±0.5 and $\rho$ = 0.3±0.05) were determined in accordance with the minimum residual condition (2):

$$\Delta(\mu_1, \mu_2, \sigma_1, \sigma_2, \rho) = \sum_{i=1}^{4}\sum_{j=1}^{4}(n_{ij} - k\,N_{ij})^2 = 9.158 \qquad (2)$$

were k is normalizing factor: $k = \sum_{i=1}^{4}\sum_{j=1}^{4} nij \;/\; \sum_{i=1}^{4}\sum_{j=1}^{4} Nij$

Binormal distribution quite well describes the statistical sequences of the occurrence frequencies of 16 types geoeffective responses which have a precursors as an interplanetary shock wave. In our approximation with increasing intensity of the magnetic storm (nGSt → sGSt → mGSt → bGSt) the part of small decreases in CR intensity (nFD and sFD) exceeds the part of moderate (mFD) and large (bFD) Forbush decreases. As a result, high value of the correlation coefficient $\rho$ = 0.88 between 16 elements $n_{ij}$ and the best approximation $N_{ij}$. The main failure of this approximation is low value of the correlation coefficient $\rho$ = 0.5.

To eliminate this failure a mathematical model of the events intensity of GSt and FD depending on two random factors of a coronal mass ejection hitting to the near-earth space was applied:

$$\mathrm{St}(Y,R) = \frac{s_0(R)}{s_{max}}\,s(Y) \quad \text{and} \quad F(Y,R) = \frac{f_0(R)}{f_{max}}\,f(Y)$$

$$\text{for} \quad s(Y) = (1-Y^2)^b \quad \text{and} \quad f(Y) = (1-Y^2)(Y+a^2)\ ,$$

were R – random variable value, which is half of the transverse dimension of the ejection; Y – relative part of R, dimensionless random variable value, which is impact parameter of the ejection relative to the Earth. The maximum values in the model ($s_0$, $f_0$) form a two-dimensional function from R, Y is a random variable with area determination (-1 ÷ 1) and (a, b) are free parameters of the model, by which one can select the spatial form of geoeffective region of the ejection according to the boundary conditions GSt (±1, R) = FD (±1, R) = 0.

Fig. 4 shows 200 values FD и GSt obtained by getting a random variable Y, which is considered uniformly distributed in the area of its determination. For the given values of a, b, $s_0$ and $f_0$ for these selections the occurrence frequencies of 16 types of virtual events different intensity Nqt ($s_0$, $f_0$; *a, b*) were calculated.

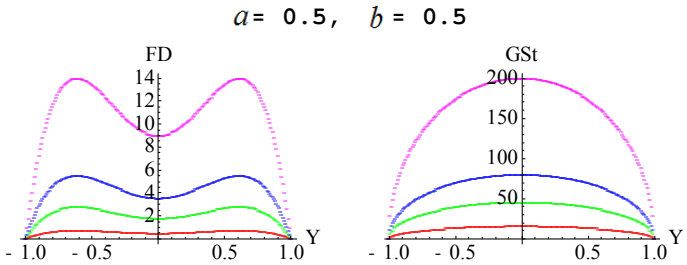


**Figure 4:** Examples of model structures FD and GSt for fixed parameters a and b. Different colors show four patterns calculated for the values $(s_0, f_0)_i = (x_i, y_i)$.

Here q and t independently of each other run character (b, m, s, n) or numeric (1, 2, 3, 4) sets. For the maximums of virtual events which were given by equality $(s_{0i}, f_{0j}) = (x_i, y_j)$ there were fulfilled calculations for 16 frequency's tables with different statistical weights determined using the formula (1). The average weighted frequencies were calculated by the expression:

$$N_{qt}(a,b,\mu_1,\mu_2,\sigma_1,\sigma_2,\rho) = \sum_{i=1}^{4}\sum_{j=1}^{4} N_{qt}\left(x_i, y_j; a, b\right)\, p\left(x_i, y_j; \mu_1, \mu_2, \sigma_1, \sigma_2, \rho\right) \quad (3)$$

Similarly for minimal residual (2) there were performed three variants of the calculation:

$$\Delta\left(a,b,\mu_1,\mu_2,\sigma_1,\sigma_2,\rho\right) = \sqrt{\sum_{i=1}^{4}\sum_{j=1}^{4}\left(n_{ij} - KN_{ij}\right)} \quad (4),$$

depending on seven free parameters under the normalization: $K = \sum_{i=1}^{4}\sum_{j=1}^{4} n_{ij} \Big/ \sum_{i=1}^{4}\sum_{j=1}^{4} N_{ij}$

Table 2 presents the calculated parameters of the General population for the four statistical modes. According to these data there were derived a qualitative evaluation of their possible contributions in generalized original selection of the events of varying intensity magnetic storms and Forbush depressions.

The calculated values of minimum residuals Δ and correlation coefficients r as shown in Fig. 3 and Fig. 5 approximations allow us to judge the representativeness of the different modes.

Table 2. The parameters of the General population for various statistical modes

| Modes | *a* | *b* | $\mu_1$, нТл | $\mu_2$, % | $\sigma_1$, нТл | $\sigma_2$, % | ρ | Δ | r |
|---|---|---|---|---|---|---|---|---|---|
| 1 | 0.4 | 0.4 | 150 | 2.5 | 100 | 9.8 | 0.7 | 5.7 | 0.95 |
| 2 | 0.4 | 0.4 | 175 | 3.5 | 100 | 7 | 0 | 7.9 | 0.91 |
| 3 | 2 | 0.5 | 150 | 2.5 | 70 | 8.4 | 0.4 | 7.5 | 0.91 |
| 4 | – | – | 150 | 2 | 91 | 3 | 0.32 | 9.2 | 0.88 |

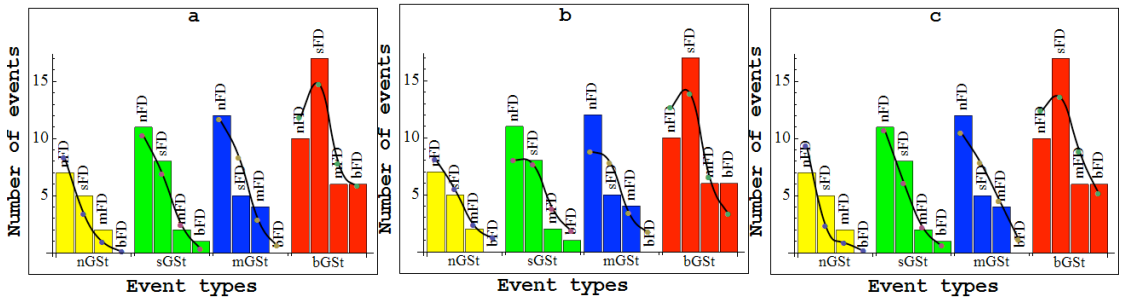


**Figure 5:** The best approximation of the histogram elements $n_{ij}$ of the matrix $N_{ij}$ , which sets were calculated using formula (3) for models GSt and FD for different values of free parameters *a*, *b,* μ1, μ2, σ1, σ2 и ρ minimizing the residual (4).

Fixed values of free parameters in two of the four variants of calculations are shown by red colors. Mode 2 for ρ = 0 applies to the case of independent components of two-dimensional

value ($s_0$, $f_0$) composed of virtual events in the model (GSt, FD). Mode 3 shown in Fig. 6c for a = 2 is consistent with cases when these maxima located in the central region of the coronal mass ejection. Comparing the values in columns of table 2 one can select mode 1 with extreme characteristics: minimum $\Delta$ = 5,7 and maximums r = 0.95 and $\rho$ = 0.7.

Thus it was found the most representative mode in original selection of geo- and helio-effects, presented by the frequency distribution in table 1. Thus the significant value of the correlation coefficient between these effects was obtained.

Using substitution $(s_0, f_0)_i = (\mu_1, \mu_2)$ in the framework of the mathematical model we calculated the mathematical expectation of the statistical mode depending on the impact parameter Y. According to the table 2 there was calculated three such dependences shown by graphs in Fig. 6.

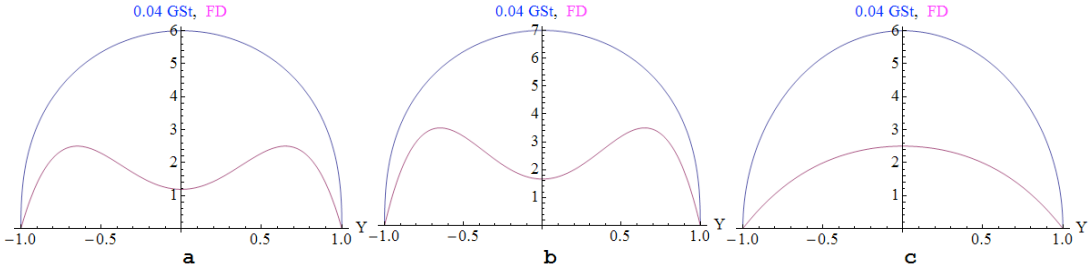


**Figure 6:** The dependences of s(Y) and f(Y) on the impact parameter Y calculated for different modes: unlimited free parameters (a); for $\rho$ = 0 (b); for a = 2 (c).

These dependencies have radical differences, due to the fact that two of them are obtained for the mode for a < 1, and the third mode for a > 1. It is possible the essence of the differences is that some f(Y) have two maximum values in the field of definition, and the other one has the only along maximum in sunflower point Y = 0.

## 4.Discussion

The fulfilled analysis of the distribution by intensity of the events in CR and Dst gives evidence that the interplanetary disturbance regions responsible for events most often do not coincide but only partially overlap, i.e. they are spaced relative to each other. The regions with low content of CR are located on the flanks of the interplanetary disturbance, and the region responsible for the magnetic storms is near the central part. Such a disposition consist with earlier results in papers [2, 12]. Different combinations the observations of ground responses to the interplanetary disturbances are caused by the geometrical factor passing of Earth through the central or flank part of the interplanetary structure.

## 5. Summary

1. Large geomagnetic storms mostly accompanied by small Forbush-effects.
2. At the beginning of the 23rd solar cycle interplanetary shocks have 16 types of the events in cosmic rays and geomagnetic field. They are indicators of comparable number of geomagnetic storms accompanied by Forbush-effects and CR decreases without storm effects.

3. The ratio of geo- and helio- effectiveness in 16 types of events is due to the fact that the region responsible for the production of the geomagnetic storms is located in the center of the interplanetary disturbance, and the region with low content of CR is shifted to its flanks.

**Acknowledgments**

This work was supported by the Russian Foundation for Basic Research, grant No.15-42-05085-r_vostok_a, by Program No.31 of the Presidium of the Russian Academy of Sciences, and by RF Presidential Grant in Support of Leading Scientific Schools NS-3269.2014.2.

## References

[1] Yermolaev Yu.I., Nikolaeva N.S., Lodkina I.G., Yermolaev M.Yu. *Relative occurrence rate and geoeffectiveness of large-scale types of the solar wind,* Cosmic Res. **48** (2010) 1-30.

[2] Shadrina L.P., Mamrukova V.P., Plotnikov I.Ya. *A combined analysis of solar-wind perturbations, cosmic-ray intensity decreases, and geomagnetic storms,* Geomag. Aeron. **36** (1996) 399-402.

[3] Badruddin. *Interplanetary shocks, magnetic clouds, stream interfaces and resulting geomagnetic disturbances,* Planet. Space Sci. **35** (1998) 1015-1028.

[4] Badruddin. *Transient modulation of cosmic ray intensity: role of magnetic clouds and turbulent interaction regions,/* Astrophys. Space Sci. **281** (2002) 651-661.

[5] Chin-Chun Wu and Lepping R.P. *Geomagnetic activity associated with magnetic clouds, magnetic cloud-like structures and interplanetary shocks for the period 1995–2003,* Adv. Space Res. **41** (2008) 335-338.

[6] Echer E. and Gonzalez W. D. *Geoeffectiveness of interplanetary shocks, magnetic clouds, sector boundary crossings and their combined occurrence,* Geophys. Res. Lett. **31** (2004) L09808.

[7] Krymsky, G.F. and Transky I.A. *The Forbush-decreases profile and convective shock waves in the interplanetary medium,* Proc. XV th ICRC. **3**. (1977) 181-185.

[8] Kudela K. and Brenkus T. *Cosmic ray decreases and geomagnetic activity: list of events 1982–2002,* J. Atmosph. Solar-Terr. Phys. **66** (2004) 1121-1126.

[9] Manoharan P. K., Gopalswamy N., Yashiro S., Lara A., Michalek G., Howard R.A. *Influence of coronal mass ejection interaction on propagation of interplanetary shocks,* J. Geoph. Res. **109** (2004) A06109.

[10] Richardson I.G. and Cane H.V. *Geoeffectiveness (Dst and Kp) of interplanetary coronal mass ejections during 1995–2009 and implications for storm forecasting,* Space Weather. **9** (2011). S07005.

[11] Papailiou M., Mavromichalaki H., Abunina M., Belov A., Eroshenko E., Yanke V., Kryakunova O. *Forbush Decreases Associated with Western Solar Sources and Geomagnetic Storms: A Study on Precursors,* Solar Phys. **283** (2013) 557-563.

[12] Shadrina L.P., Starodubtsev S.A., Plotnikov I.Ya. *Geophysical manifestations of large-scale solar wind disturbances at intersection of their flanks by the Earth,* Proc. First S–RAMP. Conf. Sapporo. (2000) 106.

[13] Takeuchi T., Russell C.T., Araki T. *Effect of the orientation of interplanetary shock on the geomagnetic sudden commencement,* J. Geophys. Res. **107** (2002) 1423-1433.

[14] Xu D., Chen T., Zhang X.X., Liu Z. *Statistical relationship between solar wind conditions and geomagnetic storms in 1998–2008,* Planet. Space Sci. **57** (2009) 1500-1513.